Study of the Higgs Production in bosonic decays channels with the CMS detector

C. Ochando
Laboratoire Leprince-Ringuet, UMR 7638, Ecole Polytechnique,
91128 Palaiseau Cedex, France

The latest results on the standard model Higgs boson studies in bosonic decays from the CMS experiment are reported. The analysis use pp collisions data recorded by the CMS detector at the LHC, corresponding to integrated luminosities up to 5.1 fb^{-1} (19.6 fb^{-1}) at $\sqrt{s} = 7$ (8) TeV. The observation of a new boson at a mass near 126 GeV is confirmed and some of its properties are shown.

1 Introduction

The standard model (SM) [1,2,3] relies on the existence of the Higgs boson (H, with mass m_H), a scalar particle associated with the field responsible for the spontaneous electroweak symmetry breaking [4,5,6,7,8,9]. In 2012, the ATLAS and CMS experiments reported the discovery a new boson at a mass around 125 GeV [10,11], compatible with the SM Higgs boson.

This letter reports the latest results from CMS with the full available statistics of the RunI of the LHC in the $H \to VV$ modes (where V stands for W, Z or γ). They have the largest sensitivity among all Higgs decays, a very good precision on the mass and can provide informations on the spin-parity state. The latter, as well as the combination of all measurements is provided elsewhere [12,13]. These proceedings focus on low mass studies (m_H <180 GeV) and only $W \to \ell\nu$ and $Z \to \ell\ell$ (where ℓ is for electron or muon) are considered.

2 H→WW→ $2\ell 2\nu$ analysis

In the H→WW→ $2\ell 2\nu$ channel [14], we search for an excess of events with two high transverse momenta (p_T) leptons of opposite charge and large missing transverse momentum (E_T^{miss}) due to undetected neutrinos. As no mass peak can be fully reconstructed, a precise control of the backgrounds is mandatory. The main one originates from non-resonant WW production. Additional contributions arise from Drell-Yan, top quark as well as W+jets or diboson processes (WZ, $W\gamma^{(*)}$, ZZ).

The event sample is split into categories of different background composition and signal-to- background ratios: same-flavor (SF) and different-flavor (DF) leptons, events with zero or one jet [a]. The reconstructed transverse mass (m_T) distribution is shown on Fig. 1 (left) for the DF category and in the 0-jet bin. A broad excess of events, compatible with the production of Higgs boson with m_H =125 GeV, can be appreciated.

The final result is extracted using a two-dimensional ($m_{\ell\ell}$, m_T)[b] shape analysis for events belonging to the DF category, and by a cut-based approach for the events falling into the SF category. The observed (expected) significance is 4.0 (5.1) standard deviations (σ) for m_H =125 GeV, as shown in Fig. 1 (right). The signal strength μ_{SM}, relative to the expectation for the SM Higgs boson, is measured to be $\mu_{SM} = 0.76 \pm 0.21$ at 125 GeV.

[a] The category with at least two jets, dedicated to the Vector Boson Fusion (VBF) production mode, was not updated in time for this conference.

[b] $m_{\ell\ell}$ is the invariant mass of the dilepton pair, m_T is the transverse mass reconstructed from the transverse momentum

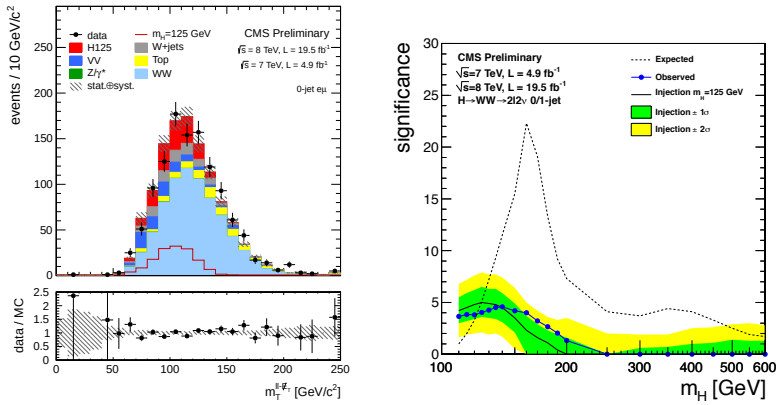

Figure 1: Distribution of the transverse mass m_T for the DF category and 0-jet bin (left). Observed (blue) and expected (dashed) statistical significance as a function of m_H (right). The expected significance (black) under the presence of a m_H=125 GeV Higgs is also shown.

3 H$\rightarrow ZZ \rightarrow 4\ell$ analysis

The H$\rightarrow ZZ \rightarrow 4\ell$ analysis [15] exhibits a clean experimental signature consisting of a narrow resonance over a small continuum background. The mass peak is built from four primary isolated and identified leptons. As low signal yields are expected, this channel critically relies on the performances of the leptons reconstruction and selection algorithms. The dominant irreducible background is from non-resonant ZZ (or Zγ^*) production. It is estimated from simulation. Additional reducible background sources arise from $Zb\bar{b}$, $t\bar{t}$, $Z+$ jets or $WZ+$ jets events where at least one jet is misidentified as lepton. It is estimated from real data.

The reconstructed four-lepton invariant-mass (m_{4l}) distribution is shown on Fig. 2 (left). A clear peak around $m_{4\ell} = 126$ GeV is seen. A matrix element likelihood approach [16,17,18] is used to build a kinematic discriminant (K_D) so as to further improve the separation between signal and background. To enhance the sensitivity to the production mechanisms, the event sample is split into two categories based on the jet multiplicity: events with fewer than two jets (C1) and events with at least two jets (C2).

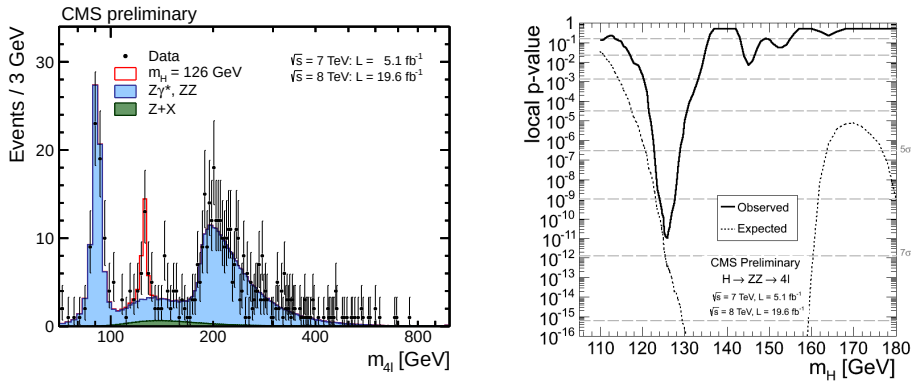

Figure 2: Distribution of the four-lepton reconstructed mass (left).Points represent the data, shaded histograms represent the background and the unshaded histogram the signal expectation. Expected (dashed) and observed (solid) local p-values (right) as a function of the Higgs boson mass.

The final result is extracted using a three dimensional model ($m_{4\ell}$, K_D, X) where X is $p_T/m_{4\ell}$ in C1 and a linear discriminant formed combining VBF sensitive variables in C2. The local p-values, representing the significance of local excesses relative to the background expectation are shown on Fig. 2 (right). The minimum is reached around $m_{4\ell} = 125.8$ GeV and corresponds to an observed (expected) local significance of 6.7 (7.1) σ. The signal strength μ_{SM} is measured to be $\mu_{SM} = 0.91^{+0.30}_{-0.24}$ at 125.8 GeV.

of the dilepton pair and the E_T^{miss} vector.

4 H→ $\gamma\gamma$ analysis

The H→ $\gamma\gamma$ analysis[19] searches for a narrow peak built from two high p_T photons over a smoothly falling background due to QCD prompt diphoton production and to events with at least on jet misidentified as photon.

To increase the sensitivity, events are separated into mutually exclusive classes: diphoton events without any tagging object (untagged), diphoton events with jets consistent with the VBF topology, and diphoton events with leptons or large E_T^{miss}, consistent with W/Z associated production (VH).

Two analyses are presented: one uses Multi-Variate-Analysis (MVA) techniques for both the photon identification and the event classification for untagged or VBF-like classes while the other is using cut-based approaches. The MVA classifier for the untagged category uses as input an event-by-event estimate of the diphoton mass resolution, a photon identification score for each photon, and kinematic informations about the photons and the diphoton system. Being the most sensitive, the MVA analysis results are taken as baseline. The background in the signal region is estimated from fits to each of the observed diphoton mass distributions in data.

The weighted diphoton invariant-mass distribution is shown on Fig. 3 for both analysis. A clear peak around $m_H = 125$ GeV is seen. The local p-values are shown on Fig. 4 for both analysis. The minimum is reached around $m_H = 125$ GeV and corresponds to a local significance of 3.2 (3.9) σ for an expectation of 4.2 (3.5) σ for the MVA (cut-based) analysis. The signal strength μ_{SM} is measured to be $\mu_{SM} = 0.78^{+0.28}_{-0.26}$ ($1.11^{+0.30}_{-0.32}$) at 125 (124.5) GeV for the MVA (cut-based) analysis.

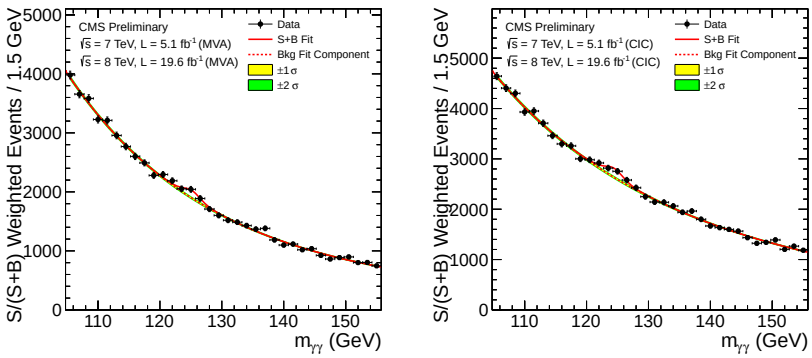

Figure 3: The diphoton mass spectrum weighted by the ratio of signal-to-background in each event class for the MVA (left) and cut-based (right) analysis.

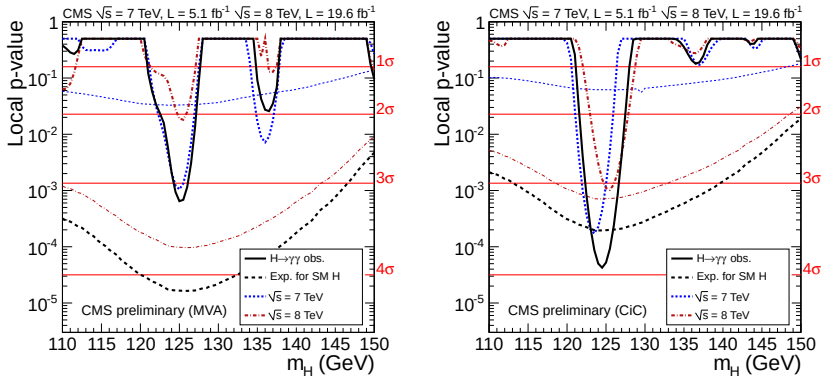

Figure 4: Expected (dashed) and observed (solid) local p-values as a function of the Higgs boson mass for the MVA (left) and cut-based (right) analysis.

5 Properties: mass and production mechanisms

The mass m_X of the observed state is measured with the high resolution channels: $ZZ \to 4\ell$ and $\gamma\gamma$. The mass and its uncertainty are extracted from one-dimensional scan of the test statistic $q(m_X)$. It is

shown on Fig. 5 (left) for the two channels separately. The resulting fit gives $m_X = 125.8 \pm 0.5$ (stat) ± 0.2 (syst) ($m_X = 125.4 \pm 0.5$ (stat) ± 0.6 (syst)) for the $ZZ \to 4\ell$ ($\gamma\gamma$) analysis.

The production mechanisms can be slit into two categories depending on whether the production is induced by vector bosons (VBF, VH) or fermions (ggH, ttH). Two signal strength modifiers (μ_V, μ_F) are introduced as scale factors to the SM expected cross section. A two-dimensional (μ_V, μ_F) fit is performed assuming the measured mass hypothesis in each channel. Fig. 5 shows the resulting fits for the $ZZ \to 4\ell$ and $\gamma\gamma$ channels. The measured values are consistent with the expectations from the production of a SM Higgs boson.

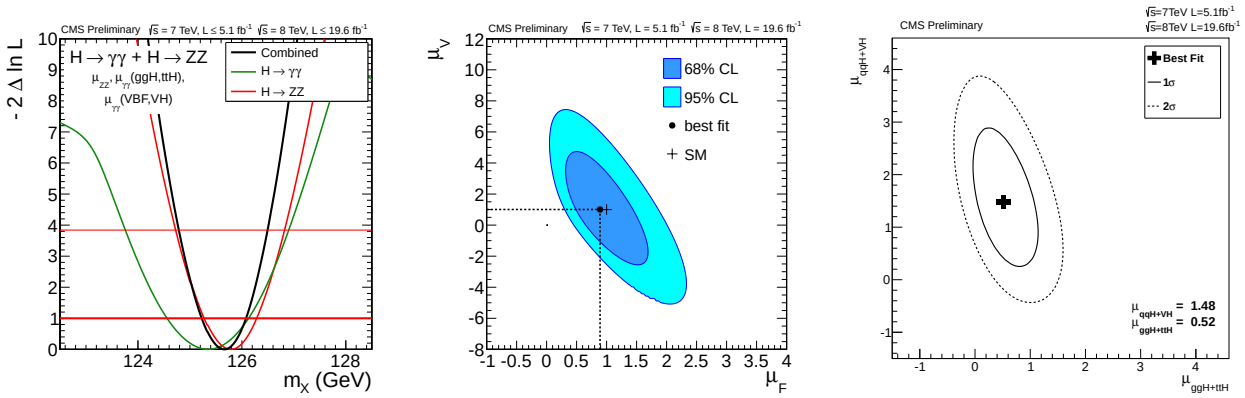

Figure 5: 1D test statistics q(m_X) $= -2\Delta lnL$ scan vs tested m_X (left) for the ZZ (red) and $\gamma\gamma$ (green) channel. Likelihood contours on the signal strength modifiers associated with fermions (μ_F) and vector bosons (μ_V) for the ZZ (middle) and $\gamma\gamma$ (right) channels.

6 Conclusion

The latest results on the standard model Higgs boson studies in bosonic decays from the CMS experiment has been presented, using data samples corresponding to integrated luminosities up to 5.1 fb^{-1} (19.6 fb^{-1}) at $\sqrt{s} = 7$ (8) TeV in pp collisions at LHC. The observation of a new boson at a mass near 126 GeV is confirmed and its properties are consistent so far with the production of a SM Higgs boson.

References

1. S. L. Glashow, Nucl. Phys. **22** (1961) 579.
2. S. Weinberg, "A Model of Leptons," Phys. Rev. Lett. **19** (1967) 1264.
3. A. Salam, in Elementary particle physics: relativistic groups and analyticity, N. Svartholm, ed., p. 367. Almqvist &Wiskell, 1968. Proceedings of the eighth Nobel symposium.
4. F. Englert and R. Brout, Phys. Rev. Lett. **13** (1964) 321.
5. P. W. Higgs, Phys. Lett. **12** (1964) 132.
6. P. W. Higgs, Phys. Rev. Lett. **13** (1964) 508.
7. G. S. Guralnik, C. R. Hagen and T. W. B. Kibble, Phys. Rev. Lett. **13** (1964) 585.
8. P. W. Higgs, Phys. Rev. **145** (1966) 1156.
9. T. W. B. Kibble, Phys. Rev. **155** (1967) 1554.
10. S. Chatrchyan *et al.* [CMS Collaboration], Phys. Lett. B **716** (2012) 30.
11. G. Aad *et al.* [ATLAS Collaboration], Phys. Lett. B **716** (2012) 1.
12. CMS Collaboration, CMS-PAS-HIG-13-005 (2013).
13. A. Whitbeck, these proceedings.
14. CMS Collaboration, CMS-PAS-HIG-13-003 (2013).
15. CMS Collaboration, CMS-PAS-HIG-13-002 (2013).
16. Y. Gao et al., Phys. Rev. D **81** (2010) 075022
17. S. Bolognesi et al., Phys. Rev. D **86** (2012) 095031
18. P. Avery et al., arXiv:1210.0896 [hep-ph].
19. CMS Collaboration, CMS-PAS-HIG-13-001 (2013).